

Toxicology Research

Accepted Manuscript



This is an *Accepted Manuscript*, which has been through the Royal Society of Chemistry peer review process and has been accepted for publication.

Accepted Manuscripts are published online shortly after acceptance, before technical editing, formatting and proof reading. Using this free service, authors can make their results available to the community, in citable form, before we publish the edited article. We will replace this *Accepted Manuscript* with the edited and formatted *Advance Article* as soon as it is available.

You can find more information about *Accepted Manuscripts* in the [Information for Authors](#).

Please note that technical editing may introduce minor changes to the text and/or graphics, which may alter content. The journal's standard [Terms & Conditions](#) and the [Ethical guidelines](#) still apply. In no event shall the Royal Society of Chemistry be held responsible for any errors or omissions in this *Accepted Manuscript* or any consequences arising from the use of any information it contains.

Cytotoxic effects and cellular oxidative mechanisms of metallic nanoparticles on renal tubular cells: Impact of particle solubility

Igor Pujalté^a, Isabelle Passagne^a, Richard Dalcusi^b, Caroline de Portal^c, Céline Ohayon-Courtès^c, Béatrice L'Azou^{a,b*}

^aPharmacochimie FRE3390, Université de Bordeaux, 146 rue Léo-Saignat, 33 076 Bordeaux Cedex, France

^bINSERM U1026, Université de Bordeaux, Bioingénierie Tissulaire BIOTIS, 146 rue Léo-Saignat, 33 076 Bordeaux Cedex, France

^cLaboratoire Hydrologie Environnement, Université de Bordeaux, 146 rue Léo-Saignat, 33 076 Bordeaux Cedex, France

*Corresponding author

Béatrice L'Azou : INSERM U1026, Université de Bordeaux, BIOTIS, 146 rue Léo-Saignat, 33 076 Bordeaux Cedex, France

Phone : + 33 5 57 57 15 20

Email : beatrice.lazou@u-bordeaux.fr

Abstract

Many uncertainties remain regarding the potential toxic effect of nanoparticles (NPs). NPs could cross biological barriers, be carried in blood to kidneys and damage renal cells. Yet, there is little data regarding NPs nephrotoxicity. The aim of this study was to understand the cytotoxic mechanisms induced by metallic NPs with different solubility properties (TiO₂, ZnO, CdS). Studies were performed *in vitro* on human epithelial tubular cells (HK-2). Cellular and molecular were investigated through oxidative stress status. By WST-1 assay it was found that cytotoxicity of NPs was dependent on particle size and metal solubility. Exposure to soluble CdS and ZnO NPs led to cell death in a dose-dependent manner related to release of metallic cations (Cd²⁺ and Zn²⁺). Insoluble TiO₂ NPs had no cytotoxic effect. Analysis of ROS production and lipid peroxidation clearly indicated the involvement of oxidative stress in cell toxicity. Soluble ZnO and CdS NPs caused lysosomal membrane destabilization (acridine orange), and nuclear condensation (DAPI). A molecular approach was used for signaling pathways. ZnO and CdS NPs induced translocation of Nrf2 and NF-κB, and induction of antioxidant enzymes. TiO₂ NPs did not cause lysosomal membrane destabilization or nuclear condensation. TiO₂ NPs slightly activated Nrf2 nuclear but no significant NF-κB nuclear translocation was observed. For TiO₂, oxidative stress was not sufficient to trigger membrane disruption. This study provides additional knowledge about the renal toxicity of NPs. Release of metal ion represented an important factor for determining toxicity. This *in vitro* assay constitutes an additional step in nanomaterial safety assessment.

Introduction

Owing to the wide and growing number of applications of nanoparticles (NPs), there is a need to investigate their biological effects and impact on human health. The attractive properties of nanomaterial included their small size, large surface area, and high reactivity. However, these may contribute to the toxicological profile of NPs in biological systems, as observed from *in vivo* and *in vitro* studies comparing NPs with their fine counterparts^{1, 2}. Due to their small size NPs can translocate to the blood stream resulting in systemic distribution all over the body. Additionally, their nanosize can facilitate cellular uptake and trigger injurious response. Studies on the biological effects of NPs were often focused on pulmonary toxicity. However, their potential effects could be different depending of cell type. There have been a limited number of studies

assessing the renal toxicity of metallic NPs although kidneys can be considered as secondary major sites after inhalation, ingestion or injection and circulation in the blood stream^{3, 4}. Furthermore, owing to high blood supply, kidneys have the ability to concentrate NPs, and in particular metallic NPs. The influence of NP size or surface treatment on renal tissue distribution has been investigated *in vivo*, and it was reported that metallic NPs distributed in the kidneys could cause damage to the glomerular and/or tubular regions⁵⁻⁸. Acute toxicity with kidney injuries has been observed with TiO₂ NPs after oral and intraperitoneal administration in mice^{9,10}. Moreover, exposure to other metallic NPs clearly led to renal cell damage as reflected by altered blood biochemical indexes, in particular noticeable changes in urea, nitrogen, and creatinine levels^{11,12}.

Metallic NPs are widely used not only in industry and medicine but also in various consumer products such as cosmetics, sunscreens, textiles, and food products¹³. For instance, TiO₂ NPs have excellent optical performance and electrical properties, and are produced for applications in paints and coatings but also in cosmetics where they are used as a UV-absorber. ZnO NPs are widely used as polymer fillers, UV absorbers but also used as antibacterial and antifungal-agents when incorporated into materials such as surface coatings (paints), textiles, and plastics. Cadmium is used in the construction of quantum dots (QDs), which are semiconductor metalloid crystal structures that have unique optical and electronic properties. QDs distribution in the kidney have been reported^{11, 14, 15}. Because shells and coatings of QDs can be degraded, their cadmium content can be released and induce renal cell damage. In previous studies we have investigated the cytotoxicity of TiO₂, ZnO, and CdS NPs in glomerular and tubular cell lines^{16,17} and we found differences in cytotoxicity that was dependent on NP metal composition but also on cell type. However, solubility may also be an important factor to consider, as it was already established that the ionized form of metals is responsible for the cellular toxicity¹⁸⁻²¹. In addition, it was reported that dissolution of ZnO NPs and Zn²⁺ release was capable of ROS generation and activation of cytotoxic pathways²². Previous studies on NP toxicity have also reported that ROS formation and oxidative stress, which induced a wide variety of cellular events, such as induction of antioxidant enzymes, oxidative damage and apoptosis, are among the most important toxic mechanisms related to NP exposure²³⁻²⁶. The modification of intracellular redox potential is generally associated with activation of ubiquitous transcription factors^{27,28}. Nuclear factor kappaB (NF-κB), activated by oxidative stress, induces the expression of a variety of proteins that function in the immunological and cellular detoxifying defense system, regulated by the intracellular redox status²⁹. When activated by oxidative stress, nuclear factor-E2-related factor-2 (Nrf2) breaks free from Keap1 and translocates into the nucleus, where it binds to an antioxidant responses element (ARE), a

cis-acting enhancer sequence that mediates the transcriptional activation of genes in response to oxidative stress, including Heme oxygenase (HO-1) Superoxide dismutase (SOD-1) or catalase (CAT)³⁰.

The current study aimed to investigate the cytotoxic mechanisms induced *in vitro* on a renal cell line by metallic NPs and focuses on TiO₂, ZnO, and CdS that have different solubility. We first determined the solubility and cytotoxicity of the NPs tested and then investigated the cellular damages related with oxidative stress induction. Oxidative stress was evaluated by increase of reactive oxygen species (ROS) production and lipid peroxidation, lysosomal membrane destabilization, and nuclear morphological modifications. To understand the molecular mechanism of NPs-induced oxidative stress, we investigated antioxidant gene transcription (OH-1, SOD, CAT, glutathion peroxidase Gpx, glutathione transferase GST-pi, thioredoxin reductase TRNX-R) and redox-sensitive transcription factor, such as Nrf2 and (NF-κB). For this *in vitro* study, assays were conducted on the human proximal epithelial tubular cell line HK-2. Owing to the physiological role of tubular cells by active and passive cell transport of metabolism products and xenobiotics, these cells were involved in intensive accumulation. Additionally, this line was widely used in the *in vitro* study of tubular damage and has proved useful in the study of different nephrotoxic xenobiotics³¹⁻³³.

Results

NPs Characterization

Differences in the characteristics of particles have been shown to play important role in NP toxicity. Thus, physicochemical parameters were assessed before experiments. The properties of certain NPs have previously been described and are summarized in Table 1¹⁷. Particle average diameters were determined using transmission electron microscope fitted with a camera and using ImageJ software. Particles were calculated with a diameter of $12,2 \pm 2.2$ nm and 200 ± 7 nm for TiO₂ NPs and μ Ps, 75 ± 19 nm and 420 ± 200 nm for ZnO NPs and μ Ps, 8 ± 1 nm and 1045 ± 44 nm for CdS NPs and μ Ps, respectively. Additionally, NP solubility was measured using optical emission spectrometry ICP-OES after 0 and 24 h in RPMI medium (Figure 1). Immediately after NP solution preparation (0 h), ZnO NPs and CdS NPs were found to be partially soluble at the concentration used. The proportion of dissolved Zn at 16 μ g/ml was 27 % (4.3 μ g/ml) at 0 h, and was 33 % (5.2 μ g/ml) after 24 h; a plateau was reached from 8 μ g/ml. The proportion of dissolved CdS at the highest concentration (16 μ g/ml) was 6 % at 0 h and was 9 % after 24 h. TiO₂ NPs were insoluble at both 0 and 24 h.

Cell Cytotoxicity – Effect of NPs solubility

Investigation of the cytotoxic effects of TiO₂, ZnO, and CdS NPs on HK-2 cells and comparison with micro and soluble forms allows a better understanding of the physicochemical parameters involved in NP toxicity. Nano- (ZnO NPs), micro- (ZnO μPs), and soluble (ZnCl₂) forms of zinc element induced cell mortality with close cytotoxicity curves. IC₅₀ were 3.4 ± 0.4 μg/cm² for ZnO NPs, 5.03 ± 0.4 μg/cm² for ZnO μPs, and 4.2 ± 0.2 μg/cm² for ZnCl₂, which suggests that nanoscale was not involved in ZnO toxicity (Figure 2A).

To determine whether the observed cytotoxicity was due to cation release in the culture medium, the same experiment was performed in the presence of EDTA (Ethylenediaminetetraacetic acid). The latter is chelating agent with affinity for divalent cations, which after being bound by EDTA, remain in solution but exhibit diminished reactivity. ZnO NP toxicity was lowered after Zn²⁺ chelation by EDTA. At 5 μg/cm² cell mortality was decreased from 67.5 ± 2.5 % to -2.6 ± 3.2 % (Figure 2B), which strongly suggests the involvement of metal cations (Zn²⁺) in cytotoxicity and confirmed the important role of Zn solubility.

For CdS, cell mortality was observed for CdS NPs but not for CdS μPs after 24 h exposure, which confirmed the importance of size in cytotoxicity. A higher toxicity was observed with soluble CdO compared to CdS (Figure 2C), which could be explained by a greater release of Cd²⁺ ions by CdO that was soluble at the concentrations used whereas CdS NPs were partially soluble, as shown previously (Figure 1). CdS NP toxicity was lowered after Cd²⁺ chelation with EDTA; at 7 μg/cm² cell mortality was decreased from 52.8 ± 3.2 % to 12.9 ± 7.2 % (Figure 2D), which strongly suggests involvement of metal cations (Cd²⁺) in CdS NP toxicity. Absence of CdS μPs toxicity was due to a lower solubility of this compound compared to CdS NPs. For TiO₂, neither NPs nor μPs induced cytotoxic effects when exposed for 24 h (Figure 2E), which can be explained by the insolubility of these particles.

Oxydative Stress

ROS Production: The ability of NPs to induce intracellular ROS production in HK-2 cells was assessed using DCFH, which reacts with hydroxyl radical and is transformed to a highly fluorescent compound DCF. All NPs tested induced an increase of intracellular ROS production: CdS NPs were the most reactive reaching 161 ± 16 % fluorescence intensity of control at the lowest concentration (5 μg/ cm²); TiO₂ and ZnO NPs reached 124 ± 12 % and 139 ± 18 % fluorescence intensity of control, respectively, at the highest concentration (20 μg/ cm²; Figure 3A).

These results suggested that ROS formation was associated with NP cytotoxicity. To confirm this hypothesis an antioxidant, N-acetylcysteine (NAC), was co-incubated with cells exposed to NPs and cell cytotoxicity investigated. NAC significantly reduced cell mortality induced by 10 $\mu\text{g}/\text{cm}^2$ ZnO NPs from $80 \pm 2 \%$ to $13 \pm 7 \%$ (Figure 3B), and 7 $\mu\text{g}/\text{cm}^2$ CdS NPs from $63 \pm 3 \%$ to $16 \pm 3 \%$ (Figure 3C); TiO₂ NPs were not investigated as these, were not found to be cytotoxic (see above).

Lipid peroxidation: Cellular oxidative damage was assessed via lipid peroxidation, which leads to malondialdehyde (MDA) formation. MDA concentration was $128 \pm 15 \mu\text{M}$ of MDA/mg protein in control cells and $506 \pm 85 \mu\text{M}$ MDA/mg protein after incubation with TBHP (Tert-Butyl Hydroperoxide) (50 μM), a positive control. In the presence of TiO₂ NPs (20 $\mu\text{g}/\text{cm}^2$) MDA concentration was $260 \pm 40 \mu\text{M}$ MDA/mg protein, in the presence of ZnO NPs (2 $\mu\text{g}/\text{cm}^2$) this was $263 \pm 22 \mu\text{M}$, and in the presence of CdS NPs (5 $\mu\text{g}/\text{cm}^2$) this was $226 \pm 23 \mu\text{M}$ (Figure 4). These results indicate that the tested NPs can cause lipid oxidative damage but that this is not correlated with cytotoxic effects as a similar effect was found for TiO₂ NPs.

Lysosomal membrane destabilization: Increased ROS production has been associated with lysosomal membrane destabilization. The ability of NPs to damage lysosomal membrane was assessed using acridine orange (AO) fluorochrome. In control cells, lysosomes (red-orange granules) can be clearly seen within the cytosol (Figure 5A). Exposure to CdS (5 $\mu\text{g}/\text{cm}^2$) and ZnO (2 $\mu\text{g}/\text{cm}^2$) NPs induced pronounced lysosomal membrane destabilization as evidence by release of lysosomal content into the cytoplasm (Figure 5A). Quantification by spectrofluorimetry confirmed this observation. Fluorescence ratio significantly ($p < 0.05$) increased in cells treated with TBHP (50 μM), positive control, to $170 \pm 19 \%$ of control, in cells treated with ZnO NPs to $140 \pm 13 \%$, and with CdS NPs to $155 \pm 13 \%$. Cells treated with TiO₂ NPs (20 $\mu\text{g}/\text{cm}^2$) showed no discharge of lysosomal content (Figure 5A), and there was no significant difference in fluorescence ratio with respect to control conditions (Figure 5B).

Cellular responses to NPs

Nuclear fragmentation: The modification of redox status and release of lysosomal contents into the cytoplasm can initiate apoptotic cell state, which was investigated using DAPI to visualize nuclear condensation. In control conditions, a negligible percentage of cells showed a condensed nucleus and the morphology of the nuclei remained unchanged upon exposure to TiO₂ NPs (20 $\mu\text{g}/\text{cm}^2$; Figure 6A). Cells exposed to CdS (6.3

$\mu\text{g}/\text{cm}^2$) and ZnO ($2 \mu\text{g}/\text{cm}^2$) NPs, showed nuclear condensation characteristic of apoptosis. This state was confirmed by a significant increase in the number of apoptotic cells (Figure 6B).

Nrf2 and NF- κ B translocation: The transcription factors Nrf2 and NF- κ B were known being activated in cells during oxidative stress. Upon exposure to the NPs tested there was a significant increase of Nrf2 protein in the nucleus ($p < 0.05$). After 1 and 4 h of ZnO NP exposure ($2 \mu\text{g}/\text{cm}^2$) nuclear protein levels were respectively $320 \pm 46 \%$ and $303 \pm 64 \%$ of control, after 1 and 4 h of CdS NP exposure ($5 \mu\text{g}/\text{cm}^2$) these levels were respectively $312 \pm 54 \%$ and $254 \pm 60 \%$. For TiO_2 NPs nuclear Nrf2 protein levels were lower than that found for other NPs but were significantly higher than control; after 1 and 4 h of TiO_2 NP exposure ($20 \mu\text{g}/\text{cm}^2$) nuclear protein levels were 165 ± 58 and 248 ± 50 . These results indicated Nrf2 translocation confirming induction of cellular antioxidant systems (Figure 7A).

In most cells NF- κ B, is present as a latent, inactive, I κ B-bound complex in the cytoplasm. When cells receive extracellular signals, NF- κ B rapidly enters the nucleus and activates gene expression. After 1 and 4 h of ZnO NP exposure ($2 \mu\text{g}/\text{cm}^2$), nuclear protein levels were respectively $366 \pm 44 \%$ and $412 \pm 35 \%$ of control. After 1 and 4 h of CdS NPs exposure ($5 \mu\text{g}/\text{cm}^2$), these levels were $80 \pm 19 \%$ and $345 \pm 66 \%$, respectively; all values were significantly higher than control ($p < 0.05$). These results indicated that the transcription factor NF- κ B was rapidly (1 h and 4 h) and strongly activated when exposed to ZnO and CdS NPs. In contrast there was no significant NF- κ B nuclear translocation in cells exposed to TiO_2 NPs (Figure 7B).

Antioxidant responses: Activation of these transcription factors allows the expression of genes involved in antioxidant responses. The transcription levels of genes encoding catalase (CAT), heme oxygenase (HO-1) and glutathione peroxidase (GPX), superoxide dismutase (SOD), glutathion transferase (GST), and thioredoxinreductase (TRNX) were investigated and found to be significantly increased for all NPs tested ($p < 0.05$). After exposure to ZnO NPs the transcription level of CAT was $375 \pm 93 \%$ of control, that of HO-1 was $379 \pm 47 \%$, and that of GPX-1 was $387 \pm 67 \%$; after exposure to CdS NPs, the transcription level of CAT was $408 \pm 60 \%$ that of HO-1 was $545 \pm 102 \%$, and that of GPX-1 was $406 \pm 74 \%$. A similar 3 to 4 -fold increase was found after exposure to CdS NPs; after TiO_2 NP exposure a 2-fold increase was observed ($188 \pm 12 \%$, $175 \pm 22 \%$ and $164 \pm 14 \%$ for CAT, HO-1 and GPX-1, respectively).

Discussion

The aim of this study was to understand the cytotoxic mechanisms induced by metallic NPs with different solubility properties on the kidney. The nanosize of such particles provides them the ability to cross biological barriers and to be distributed throughout the body^{6, 34}. After translocation, NPs which generated biological reactivity can contribute to kidney damage and promote lesions or disease^{12, 35}. However, the diagnosis of kidney disease is often difficult; 70 % of nephron potential must be injured before observation of first clinical signs of renal failure. Thus, a better understanding of the renal effects of NPs is required to notify of potential kidney damage. Using kidney cells in culture allows a rapid and efficient screening of toxic effects induced *in vitro* by NPs and provides an understanding of the cellular and molecular mechanisms involved. The literature indicates that the three types of metal NPs used in this study (TiO₂, CdS and ZnO) have the ability to distribute in the kidney after *in vivo* administration^{10, 14, 36, 37}. However, there is limited knowledge concerning the toxicological effects of NPs on the kidney, except that it is now known that the toxic behavior of NPs differ from their bulk counterparts.

The present study demonstrates that zinc, ZnO NPs as well as ZnO μ Ps were toxic on HK-2 tubular cells at very low concentrations and that there was no difference attributable to particle size as IC₅₀ values were not significantly different. Interestingly, cytotoxicity curves of ZnO particles were closed to that of a soluble form of Zn (ZnCl₂). Consequently, the ZnO toxicity could be attributed to dissolved Zn. Measurement of Zn²⁺ in an acellular model found that ZnO NPs were the most soluble of the NPs tested. Moreover, deprivation of Zn²⁺ cations by adding EDTA nullled the observed cytotoxicity of ZnO NPs. This strongly suggests that the released metal cations (Zn²⁺) were at the origin of cytotoxicity, which is in accordance with Kasemets K. *et al.*³⁸ who report that micro- and nano-particulates forms of zinc are toxic, not according to the size or scale of particles, but rather on the availability and amount Zn²⁺ ion released. The effect of solubility on NP toxicity was highlighted by Brunner *et al.*³⁹, where insoluble NPs (TiO₂, CeO₂, and ZrO₂) induced fewer cytotoxic effects than soluble or partially soluble NPs (ZnO, Fe₂O₃, and Ca₃(PO₄)₂). Furthermore, it has also been demonstrated that the cytotoxic effects of ZnO particles were related to intra and extracellular particle dissolution²⁰. ZnO NPs rapidly dissolve under acid conditions and this did not differ with the size of particles Cho *et al.*,⁴⁰. For cadmium, it has been suggested that their toxicity was size dependant. It has been shown that CdS QD cytotoxicity is greater than micro-sized CdS¹⁹. As suggested by the authors, Cd²⁺ release could promote toxic

effects, and in the present study, we observed that cationic deprivation of CdS NPs led to an important reduction of toxicity at a NP concentration higher than the IC₅₀. Certain authors have reported that nearly 20 % of free cadmium was released from CdS QD in cells¹⁹, and we speculate that the size could influence release of Cd²⁺, explaining low solubility of CdS μ Ps. The high solubility of certain NPs could be explained by their composition and their intracellular localization. Authors suggested that the source of free metal comes from release from phagolysosomes⁴¹, and dissolution may be caused by the acid milieu of lysosomes leading to lysosomal damage as was observed in present study. In contrast to ZnO and CdS NPs, TiO₂ NPs induced low toxicity, probably due to their insolubility, even in this acid environment. Moreover, no lysosomal alteration was observed in cells treated with TiO₂.

The larger surface area per mass of NPs could increase surface-dependant reactions such as ROS production. Moreover, Cd²⁺ and Zn²⁺ ions could be directly at the origin of this oxidative stress. For instance, Cd²⁺ can replace physiological metal and thus increase the amount of free metal such as iron and copper that participate in ROS generation via Fenton reactions⁴². Cd²⁺ was also known for its disruptive effects on physiological functions, resulting from increased levels of ROS, oxidation of thiol groups or direct damage to transport enzymes, etc.^{43, 44}. Lysosomal membrane destabilization can be triggered by an increase of intracellular ROS and in consequence release of lysosomal contents into the cytosol, that was considered as an important step in apoptosis induction⁴⁵. The release of lysosomal content and cytosol acidification contribute to caspase activation⁴⁶ and facilitate dimerization of pro-apoptotic members of Bcl-2 family⁴⁷. We observed that the most soluble NPs were a major source of lysosomal destabilization and this result was associated with important nuclear condensation confirming cellular apoptosis. Compared to TiO₂ NPs, ZnO and CdS NPs effectively induced an increase of intracellular ROS levels at low concentrations, and co-Incubation with antioxidants confirmed that ROS formation were responsible for toxic effects. These results were in accordance with an *in vivo* study reported by Shaikh et al.⁴⁸ where an antioxidant (N-acetylcysteine, or vitamin E) prevented lipid peroxidation induced by Cd and protected animals against renal and hepatic toxicity. ROS formation can exceed cellular defensive capacity and induce oxidative stress that is associated with biomolecular damage (including lipids, proteins, and DNA)⁴⁹. Release of Cd²⁺ has been described to initiate lipid peroxidation and disrupt membrane composition⁵⁰, and Li *et al.*¹⁹ have previously suspected intracellular ROS production, GSH depletion and release of Cd²⁺ ions, as the main toxic mechanism in CHL cells exposed to CdS NPs. Other studies using Cd NPs or QDs have also found similar results: ROS production, decrease in the GSH/ GSSG ratio^{19, 51}, and

cell viability^{52, 53}, associated with Cd²⁺ release. Our results were also consistent with the effects of Zn²⁺ described in the literature, *i.e.* increased of ROS and lipid peroxidation, decrease of cell viability⁵⁴⁻⁵⁶. In our study, the increased in ROS level was associated with a concomitant elevation of malondialdehyde (MDA) which reflects lipid peroxidation.

Increased transcription of antioxidant genes (Catalase, Heme Oxygenase - HO-1, Gutathione Peroxidase - GPX, Superoxide Dismutase - SOD, Glutathione S-Transferase - GST, and Thioredoxin Reductase - TRNX-R) was observed at lower concentrations of ZnO and CdS NPs. This result was associated with nuclear Nrf2 translocation that is the major transcription factor that regulates the antioxidant response in order to combat toxic effects and which is activated in response to cellular oxidative imbalance generated by exogenous and endogenous substances, metals, and radiation²¹. After exposure to ZnO and CdS NPs, the NF-κB transcription factor was also translocated to the nucleus. NF-κB is known as a transcription factor sensitive to oxidative status of cell and involved in the restoration of redox homeostasis^{39, 42}. NF-κB transcription factor mainly plays a crucial role in the regulation of genes encoding pro-inflammatory cytokines, leading to inflammation process. However, it may partially participate to the induction of genes involved in antioxidant response, such as, the expression of SOD and HO-1. SOD is a well-characterized primary enzyme for ROS scavenging, whereas HO-1 was a relatively novel enzyme, with potent anti-inflammatory and cytoprotective antioxidant effects. This activation of cellular defense mechanisms promotes short-term protection of proximal tubular cells, triggering pro-inflammatory and antioxidant response involved in an anti-apoptotic effect. Whereas Nrf2 is known to confer cell protection, NF-κB may also be implicated in deleterious effects. Moreover, it has been reported that NF-κB can repress Nrf2 signaling⁵⁷. We can suppose that nuclear translocation of NF-κB with ZnO and CdS NPs could participate to an overtaking of antioxidant cellular defense. In the present study, TiO₂ NPs did not induce NF-κB translocation, which may confirm their low toxicity. Similar results were observed by Eom *et al.*⁵⁸, where CeO₂ NPs induced a low cytotoxic effect, an antioxidant response that involved the nuclear translocation of Nrf2, but absence of translocation of NF-κB. TiO₂ NPs have the ability to generate intracellular ROS and to activate Nrf2, but the oxidative stress was not sufficient to disrupt the redox balance, thus preventing emergence of cytotoxic effect. Moreover the increase of ROS was not associated with damage lysosomal membrane. No significant decrease in the ratio GSH/ GSSG has been reported¹⁷, and studies of TiO₂ suggest that ROS production is linked to the reactive surface of the particle, which depends on the size and the crystal structure⁵⁹.

At nanoscale, material acquired specific behavior, exacerbating their physicochemical properties, but also their biological reactivity. Then, it is necessary to study their impact in exposed organisms. The aim of this study was to understand the cytotoxic mechanisms induced by metallic NPs, on a secondary target organ, the kidney.

Experimental

Chemicals

NPs of TiO₂ (15 nm) and ZnO (75 nm) were purchased from Sigma Aldrich (St-Quentin-Fallavier, France). CdS NPs were manufactured by the Institute of Chemistry of Condensed Matter of Bordeaux (ICMCB, Bordeaux, France). The CdS NPs (10 nm) were prepared via a colloidal approach in aqueous solution, as previously described in Pujalté *et al.*⁶⁰. Micro-sized TiO₂ and ZnO particles were purchased from Sigma Aldrich (St-Quentin-Fallavier, France) and micro-sized CdS micro-particles from Alfa Aesar (Schiltigheim, France). CdO, was purchased from Sigma Aldrich (St-Quentin-Fallavier, France). All products used for cell culture (RPMI 1640 and DMEM/F12 media, PBS, HEPES) were purchased from Lonza (Verviers, Belgium; exceptions mentioned). WST-1 was purchased from Roche Diagnostics (Meylan, France). Trizol reagent, oligo-dT primer, MLV-reverse transcriptase and PCR (Polymerase Chain Reaction) reagents were obtained from Invitrogen (Carlsbad, CA, USA). Rabbit anti-human-NF-κB (subunit p65) was purchased from Santa Cruz BioTechnologies (Dallas, TX, USA) and other antibodies (rabbit anti-Nrf2, mouse anti-human-TBP, goat anti-rabbit or mouse-HRP) from Abcam (Cambridge, MA, USA). All other chemicals were purchased from Sigma Aldrich (St-Quentin-Fallavier, France).

Preparation and characterization of particles

Stock suspensions of micro (μP) CdS, μPs and nano (NPs) TiO₂ and ZnO particles were prepared (2 mg/ml) in RPMI 1640- serum-free medium without phenol red, L-glutamine and antibiotics. Prior to each experiment working solutions were sonicated (20s, 3 times; Vibracell 75186, 130 W, 56-60 Hz) to distribute the particles in the as evenly as possible. To directly compare compounds, usually expressed as μg/ml or μM, all NP concentrations were expressed in μg/cm² of metal element used. Several features of particles were previously investigated in RPMI 1640- serum-free medium and described in Pujalté *et al.*⁶⁰. Briefly, authors performed transmission electron microscope to determine size, shape and aggregation state. Zeta potential was assessed using a malvern Zetasizer. Additionally, in this study solubility was investigated. TiO₂, ZnO, and CdS particle suspensions were incubated for 0 or 24 h in RPMI 1640- serum-free medium at 37 °C in a humidified 5 % CO₂

environment in acellular models. Centrifugation (19 000 g for 15 min) was used to remove solid phase TiO₂, ZnO, or CdS from the complete medium. 0.4 ml of the supernatant was added to 40 µl of ultrahigh purity HNO₃ (68 %), and digested at room temperature for 24 h. Ti, Zn, and Cd content were analyzed using optical emission spectrometry ICP-OES (IRIS Intrepid IIXSP, Thermo Electron, Waltham, MA, USA). Details on instrumentation and operating conditions have previously been published⁶¹. The statistical characteristics of the calibrating function and reliability were calculated using the AFNOR method (AFNOR XP T90-210).

Cell Culture

Human Kidney (HK-2) epithelial cells were purchased from the American Type Culture Collection (ATCC, CRL-2190). Cells were grown in DMEM/F12 (Dulbecco's Modified Eagles Medium) supplemented with 2 mM L-glutamine, streptomycin (100 U/ml) and penicillin (100 µg/ml), supplemented with 10 % FBS. HK-2 cells presented morphological and functional characteristics of proximal tubular cells. The HK-2 cell line retain the characteristics of isolated normal adult proximal tubular cells and represents an alternative to primary cultures of human cells; the cell line is well differentiated on the basis of its histochemistry, immune, cytological and functional characteristics⁶²⁻⁶⁴. Cells form a monolayer and expresses biochemical properties of tubular epithelial cells. Cells were maintained in 75 cm² plastic culture flasks (Greiner BioOne, Courtaboeuf, France) in a humidified 5 % CO₂ environment. Culture medium was changed every 2 days and cells were trypsinized when necessary (0.05 % trypsin - 0.53 mM EDTA).

Cytotoxicity assays

Effects of particles on HK-2 cell viability were evaluated using the WST-1 [2-(4-iodophenyl)-3-(4-nitrophenyl)-5-(2,4-disulfophenyl)-2H-tetrazolium] assay. Mitochondrial activity was assessed via the cleavage of the tetrazolium salt to a formazan dye by succinate-tetrazolium reductase. Sub-confluent cells in 96-well plates were exposed to varying concentrations of particles for 24 h in serum-free medium. In relation to the well surface (0.32 cm²) and volume distributed (0.1 ml/well), concentrations ranging from 0.625 to 160 µg/cm², 0.1 to 20 µg/cm² and, 0.7 to 7 µg/cm², for TiO₂, ZnO, and CdS, respectively. The WST-1 reagent was added directly to culture medium for 30 minutes and absorbance was measured at λ_{450 nm} compared to a λ_{630 nm} reference using a multiscan photometer (Titertek Plus II, Labsystem). Data were expressed as percent of dead cells compared to control (100 - % of viable cells) from the same experiment obtained from at least 3 independent triplicate experiments

ROS Production

ROS production was determined in serum-free media using 20 μM of 2-7' dichlorodihydrofluorescein diacetate (DCFH-DA) and incubation for 15 min. Cells were washed with PBS and treated with different concentrations of NPs for 4 h. After exposure, cells were scraped off, lysed by sonication, and centrifuged. Supernatants were collected and ROS levels were determined at excitation $\lambda_{480 \text{ nm}}$ and emission $\lambda_{520 \text{ nm}}$ wavelengths using a fluorimeter (Kontrol Instrument, SFM 25, Eching, Germany). Data from at least 3 independent experiments are reported as proportion of fluorescence intensity and expressed as mean fluorescence ratio (fluorescence of exposed cells/fluorescence of unexposed control from the same experiment).

Lipid peroxidation using MDA quantification

This method is based on the quantification of colored complex formed between thiobarbituric acid (TBA) and malondialdehyde (MDA) after acid hydrolysis reaction. Briefly, cells were exposed 24 h to NPs (20 $\mu\text{g}/\text{cm}^2$ for TiO_2 ; 2 $\mu\text{g}/\text{cm}^2$ for ZnO and 5 $\mu\text{g}/\text{cm}^2$ for CdS) in RPMI 1640, then washed, detached by trypsinization and lysed. Thiobarbituric acid (TBA 0.55 mM, pH 7.4) and trichloroacetic acid (15 %) were mixed with an equal volume of cell lysate. The mixture was heated for 1 h, and colorimetric reaction was obtained after extraction with butanol. Absorbance was measured in a fluorimeter (Kontrol Instrument, SFM 25, excitation $\lambda_{532 \text{ nm}}$ and emission $\lambda_{553 \text{ nm}}$). Results were calculated as μM of thiobarbituric acid reactive substances from lipid peroxidation using standard solution (1, 1, 3, 3-tetramethoxypropane) and expressed in terms of MDA content as $\mu\text{M}/\text{mg}$ of protein using BioRad assay (Hercules, CA, USA) based on the Bradford method.

RNA isolation and Gene expression analysis

Cells were scrapped in trizol, and RNA extracted with chloroform, precipitated with isopropanol, and washed with absolute ethanol. Reverse-transcription polymerase chain reaction (RT-PCR) was performed using oligo deoxythymidine primer (37 °C for 50 min and 50 °C for 10 min). The RT-PCR reaction was performed with 1 μg of total RNA, 1 μl of 20 μM oligo dT primer, and 18 μl of RT-PCR PreMix. Initial denaturation was performed at 94 °C for 15 min, denaturation at 94 °C for 1 min, elongation at 72 °C for 1 min, and final elongation at 72 °C for 15 min. The hybridization conditions and the number of cycles are variable depending on the primer pair used and summarized in Table 2. Amplified cDNA products were separated on 1.5 % agarose gel by electrophoresis. The primer sequence of Actin- β mRNA was used as loading control. After revelation and gel scanning, the intensity of the bands was evaluated using ImageJ software.

Nuclear and Cellular Protein Extraction

After NP exposure, cells in 60 mm petri dishes were scraped off in ice-cold lysis buffer (Hepes 10 mM, KCl 10 mM, MgCl₂ 1.5 mM, EDTA 0.1 mM; pH 7.9) containing proteinase inhibitors (NaF 10mM, Na₃VO₄ 2 mM, DTT 0.5 mM, and 200 µl of protease inhibitor cocktails). NP40 (0.6 %) was added and lysates were centrifuged at 19000 g, 15 min at 4 °C. Supernatants (cytosolic fraction) were collected and stored at -20 °C. Pellets were lysed and resuspended in nuclear extract buffer (Hepes 10 mM, NaCl 0.4 M, EDTA 0.2 mM; pH 7.9) containing proteinase inhibitors (NaF 10mM, Na₃VO₄ 2 mM, DTT 0.5 mM and 200 µl of protease inhibitor cocktails). After incubation (4°C for 15 min) and centrifugation (19 000 g for 15 min), supernatants (nuclear fraction) were collected and stored at -20 °C. Protein contents were assessed using BioRad Bradford protein assay.

Western Blot Analysis

Western blot analysis was performed by SDS-PAGE (sodium dodecyl sulfate polyacrylamide gel). Briefly, samples were prepared in Laemmli loading buffer, and heated at 80 °C for 10 min. Samples were resolved in a vertical electrophoresis chamber (Bio-Rad) using a 10 % acrylamide resolving gel for 1.30 h at 100 V. Separated proteins were transferred to nitrocellulose membranes for 1.30 h at 100 V. Coomassie blue and Ponceau red were used to stain gels and nitrocellulose membranes in order confirm transfer. Blots were blocked overnight in 5 % skimmed milk in PBST (PBS 0.1 % Tween-20) at 4 °C. For immunoblotting, the membrane was incubated with rabbit anti-human-NF-κB (subunit p65; 1:8000) or rabbit anti-Nrf2 (1:1000) overnight in 2.5 % milk-PBST. Mouse anti-human-TBP (1:3000) antibody and anti-β-Tubulin (1:4000) were used to normalize the protein level of cytosolic and nuclear fractions (respectively). Goat anti-rabbit-HRP (1:5000) in 2.5 % milk-PBST was used to visualize NF-κB and Nrf2; Goat anti-mouse-HRP (1:2000) in 2.5 % milk-PBST was used to visualize TBP and β-Tubulin. Western Lightning™ Plus-ECL (LifeTechnology) as used according to the manufacturer's instructions and intensity of bands were calculated using ImageJ software.

Lysosomal Membrane Integrity

Lysosomal membrane integrity was performed using metachromatic fluorophore acridine orange (AO) (adapted from Sohaebuddib et al.,⁶⁵. AO diffuses into cells and accumulates in lysosomes by proton trapping. This accumulation produces a change in fluorescence emission (from cytosolic green to red) within lysosomes due to concentration-dependent stacking of the AO. Disruption of the lysosomal membrane was assessed by change in intracellular AO fluorescence. For qualitative studies, cells exposed to NPs were loaded with AO (5

µg/ml) in serum-free media for 15 min at 37 °C. After additional washing steps, culture slices were analyzed using a fluorescence microscope. For quantitative analysis, cells exposed to NPs were scrapped and cell suspensions were stained with AO (5 µg/ml). After centrifugation, supernatant was discarded and the pellet resuspended in fresh medium. AO concentration in the cell suspension was measured using a fluorescence spectrophotometer (Kontrol Instrument, SFM 25). Lysosomal membrane integrity was calculated based on the percent change in the intensity emission ratio $\lambda_{530\text{ nm}} / \lambda_{620\text{ nm}}$ (when excited at $\lambda_{495\text{ nm}}$) of treated cells with respect to the controls. TBHP (Tert-Butyl Hydroperoxide, 50 µM) was used as positive control.

DAPI staining

Cells were fixed with ice-cold paraformaldehyde (4 % in PBS) for 20 min and stained with DAPI (1 µg/ml in PBS) for 2 min. Cells were analyzed using a fluorescence microscope with appropriate filters (DAPI filter, 461 nm; LEICA DMI3000B). Cells with condensed nuclei were considered as apoptotic. Cells were photographed and the percentage of cells with apoptotic nuclei was determined (N>100).

Statistics

For cytotoxicity experiments results were calculated using the formula $(100 - (\text{Absorbance treated sample} \times 100 / \text{Absorbance control sample}))$ and expressed as mean \pm se of at least three independent experiments. Non-linear Boltzman regression analysis was performed using the Origin® software (Origin Lab. Corp, Northampton, USA) and the IC₅₀ (defined as concentration which induces 50 % cell mortality increase) were calculated. For ROS and lysosomal membrane integrity measurements, statistical analysis was performed for the experiments conducted in at least triplicate using Student's *t*-test (mean \pm se). For all experiments, the level of significance was set at **p* > 0.05.

Conclusion

The present study found that release of metal ion in solution is an important factor for determining the toxicity of NPs, and our results suggested that ZnO and CdS NPs may exert their toxicity through oxidative stress. Adaptive response in the kidney seems to borrow the same mechanisms as those described in the literature for the lung. This *in vitro* assay, performed on renal cells, constitutes an additional step in nanomaterial safety assessment.

Acknowledgments

We gratefully acknowledge Mona Treguer for synthesis of Cd NPs in the Institute of Chemistry of Condensed Matter of Bordeaux (ICMCB, Bordeaux, France)

Funding Sources

This work was funded by ANSES (*Agence Nationale de Sécurité Sanitaire de l'Alimentation, de l'Environnement et du travail*, EST 2008-22 and EST 2010/2/87).

Competing Interests

The authors declare that they have no competing interests

References

1. Oberdorster, G., Oberdorster, E. and Oberdorster, J. (2005) Nanotoxicology: an emerging discipline evolving from studies of ultrafine particles. *Environ Health Perspect.* 113:823-839.
2. Donaldson, K., Brown, D., Clouter, A., Duffin, R., Macnee, W., Renwick, L., Tran, L. and Stone, V. (2002) The pulmonary toxicology of ultrafine particles. *J Aerosol Med.* 15:213-220.

3. Nemmar, A., Hoet, P., Vanquickenborne, B., Dinsdale, D., Thomeer, M., Hoylaerts, M., Vanbilloen, H., Mortelmans, L. and Nemery, B. (2002) Passage of inhaled particles into the blood circulation in humans. *Circulation* 105:411-414.
4. Singh, S., Rahman, R., Murty, U., Mahboob, M. and Grover, P. (2013) Comparative study of genotoxicity and tissue distribution of nano and micron sized iron oxide in rats after acute oral treatment. *Toxicol Appl Pharmacol.* 266 (1):56-66.
5. Choi, C., Zuckerman, J., Webster, P. and Davis, M. (2011) Targeting kidney mesangium by nanoparticles of defined size. *Proc Natl Acad Sci U S A.* 108:6656-6661.
6. Dejong, W., Hagens, W., Krystek, P., Burger, M., Sips, A. and Geertsma, R. (2008) Particle size-dependent organ distribution of gold nanoparticles after intravenous administration. *Biomaterials* 29:1912-1919.
7. Jain, T., Reddy, M., Morales, M., Leslie-Pelecky, D. and Labhsetwar, V. (2008) Biodistribution, clearance and biocompatibility of iron oxide magnetic nanoparticles in rats. *Mol Pharm.* 5(2):306-327.
8. Yang, R., Chang, L., Wu, J., Tsai, M., Wang, H., Kuo, Y., Yeh, T., Yang, C. and Lin, P. (2007) Persistent tissue kinetics and redistribution of nanoparticles Quantum Dot 705, in mice: ICP-MS quantitative assessment. *Environ Health Perspect.* 115(9):1339-1343.
9. Chen, J., Dong, X., Zhao, J. and Tang, G. (2009) In vivo acute toxicity of titanium dioxide nanoparticles to mice after intraperitoneal injection. *J Appl Toxicol.* 29:330-337.
10. Fabian, E., Landsiedel, R., Ma-Hock, L., Wiench, K., Wohlleben, W. and Vanravenswaay, B. (2008) Tissue distribution and toxicity of intravenously administered titanium dioxide nanoparticles in rats. *Arch Toxicol.* 82:151-157.
11. Sadaf, A., Zeshan, B., Wang, Z., Zhang, R., Xu, S., Wang, C. and Cui, Y. (2012) Toxicity evaluation of hydrophilic CdTe quantum dots and CdTeSiO₂ nanoparticles in mice. *J Nanosci Nanotechnol.* 12(11):8287-92.
12. Chen, Z., Meng, H., Xing, G., Chen, C., Zhao, Y., Jia, G., T., W., Yuan, H., Ye, C., Zhao, F. and Al:, E. (2006) Acute toxicological effects of copper nanoparticles in vivo. *Toxicol Lett.* 163:109-120.
13. Piccinno, F., Gottschalk, F., Seeger, S. and Nowack, B. (2012) Industrial production quantities and uses of ten engineered nanomaterials for Europe and the world. *J Nanopart Res.* 14:1109-1120

14. Gopee, N., Roberts, D., Webb, P., Cozart, C., Siitonen, P., Warbritton, A., Yu, W., Colvin, V., Walker, N. and Howard, P. (2007) Migration of intradermally injected quantum dots to sentinel organs in mice. *Toxicol Sci.* 98:249-257.
15. Rzigalinski, B. and Strobl, J. (2009) Cadmium-containing nanoparticles: perspectives on pharmacology and toxicology of quantum dots. *Toxicol Appl Pharmacol.* 238:280-288.
16. L'azou, B., Passagne, P., Mounicou, S., Tréguer-Demapière, M., Pujalté, I., Szpunar, J., Lobinski, R. and Ohayon-Courtès, C. (2014) Comparative cytotoxicity of cadmium form (CdCl₂, CdO, CdS micro and nanoparticles) in renal cells. *Toxicol Res.* 3:32-41.
17. Pujalte, I., Passagne, I., Brouillaud, B., Treguer, M., Durand, E., Ohayon-Courtès, C. and L'azou, B. (2011) Cytotoxicity and oxidative stress induced by different metallic nanoparticles on human kidney cells. *Part Fibre Toxicol.* 8:10.
18. Barbier, O., Jacquillet, G., Tauc, M., Cougnon, M. and Pojeol, P. (2005) Effect of heavy metal on and handling by the kidney. *Nephron Physiol.* 99:105-110.
19. Li, K., Chen, J., Bai, S., Wen, X., Song, S., Yu, Q., Li, J. and Wang, Y. (2009) Intracellular oxidative stress and cadmium ions release induce cytotoxicity of unmodified cadmium sulfide quantum dots. *Toxicol In Vitro.* 23(6):1007-13.
20. Xia, T., Kovoichich, M., Liong, M., Madler, L., Gilbert, B., Shi, H., Yeh, J., Zink, J. and Nel, A. (2008) Comparison of the mechanism of toxicity of zinc oxide and cerium oxide nanoparticles based on dissolution and oxidative stress properties. *ACS Nano.* 2:2121-2134.
21. Studer, A., Limbach, L., Van Duc, L., Krumeich, F., Athanassiou, E., Gerber, L., Moch, H. and Stark, W. (2010) Nanoparticle cytotoxicity depends on intracellular solubility: comparison of stabilized copper metal and degradable copper oxide nanoparticles. *Toxicol Lett.* 197:169-174.
22. George, S., Pokhrel, S., Xia, T., Gilbert, B., Ji, Z., Schowalter, M., Rosenauer, A., Damoiseaux, R., Bradley, K., Mädler, L. and Nel, A. (2009) Use of a rapid cytotoxicity screening approach to engineer a safe zinc oxide nanoparticle through iron doping. *ACS Nano.* 4(1):15-29.
23. Moller, P., Jacobsen, N., Folkmann, J., Danielsen, P., Mikkelsen, L., Hemmingsen, J., Vesterdal, L., Forchhammer, L., Wallin, H. and Loft, S. (2010) Role of oxidative damage in toxicity of particulates. *Free Radic Res.* 44:1-46.

24. Nel, A., Xia, T., Madler, L. and Li, N. (2006) Toxic potential of materials at the nanolevel. *Science* 311:622-627.
25. Xia, T., Kovichich, M., Brant, J., Hotze, M., Sempf, J., Oberley, T., Sioutas, C., Yeh, J., Wiesner, M. and Nel, A. (2006) Comparison of the abilities of ambient and manufactured nanoparticles to induce cellular toxicity according to an oxidative stress paradigm. *Nano Lett.* 6(8):1794-807.
26. Huang, C., Aronstam, R., Chen, D. and Huang, Y. (2010) Oxidative stress, calcium homeostasis, and altered gene expression in human lung epithelial cells exposed to ZnO nanoparticles. *Toxicol In Vitro.* 24(1):45-55.
27. Leonard, S., Harris, G. and Shi, X. (2004) Metal-induced oxidative stress and signal transduction. *Free Radic Biol Med.* 37:1921-1942.
28. Unfried, K., Albrecht, C., Klotz, L., Von Mikecz, A., Grether-Beck, S. and Schins, R. (2007) Cellular responses to nanoparticles: Target structures and mechanisms. *Nanotoxicology* 1:52-71.
29. Mercurio, F. and Manning, A. (1999) NF-kappaB as a primary regulator of the stress response. *Oncogene* 18:6163-6171.
30. Lee, J., Li, J., Johnson, D., Stein, T., Kraft, A., Calkins, M., Jakel, R. and Johnson, J. (2005) Nrf2, a multi-organ protector? *FASEB J.* 19:1061-1066.
31. Hausheer, F., Ding, D., Shanmugarajah, D., Leverett, B., Huang, Q., Chen, X., Kochat, H., Ayala, P., Petluru, P. and Parker, A. (2011) Accumulation of BNP7787 in human renal proximal tubule cells. *J Pharm Sci.* 100(9):3977-3984.
32. Iwatsuki, M., Inageda, K. and Matsuoka, M. (2011) Cadmium induces phosphorylation and stabilization of c-Fos in HK-2 renal proximal tubular cells. *Toxicol Appl Pharmacol* 251(3):209-216.
33. Sanchez-Gonzalez, P., Lopez-Hernandez, F., Morales, A., Macias-Nunez, J. and Lopez-Novoa, J. (2011) Effects of deferasirox on renal function and renal epithelial cell death. *Toxicol Lett.* 203(2):154-161.
34. Hagens, W., Oomen, A., Dejong, W., Cassee, F. and Sips, A. (2007) What do we (need to) know about the kinetic properties of nanoparticles in the body? *Regul Toxicol Pharmacol* 49:217-229.
35. Wang, J. X., Zhou, G., Chen, C., Yu, H., Wang, T., Ma, Y., Jia, G., Gao, Y., Li, B., Sun, J., Li, Y., Jiao, F., Zhao, Y. and Chai, Z. (2007) Acute toxicity and biodistribution of different sized titanium dioxide particles in mice after oral administration. *Toxicol Lett.* 168(2):176-185.

36. Baek, M., Chung, H., Lee, J., Kim, T., Oh, J., Lee, W., Paek, S., Lee, J., Jeong, J., Choy, J. and Choi, S. (2012) Pharmacokinetics, tissue distribution and excretion of zinc oxide nanoparticles. *Int Nanomedecine*. 7:3031-97.
37. Trabelsi, H., Azzouz, I., Ferchichi, S., Tebourbi, O., Sakly, M. and Abdelmelek, H. (2013) Nanotoxicological evaluation of oxidative responses in rat nephrocytes induced by cadmium. *Int J Nanomedecine*. 8:3447-3453.
38. Kasemets, K., Ivask, A., Dubourguier, H. and Kahru, A. (2009) Toxicity of nanoparticles of ZnO, CuO and TiO₂ to yeast *Saccharomyces cerevisiae*. *Toxicol In Vitro*. 23:1116-1122.
39. Brunner, T., Wick, P., Manser, P., Spohn, P., Grass, R., Limbach, L., Bruinink, A. and Stark, W. (2006) In vitro cytotoxicity of oxide nanoparticles: comparison to asbestos, silica, and the effect of particle solubility. *Environ Sci Technol* 40:4374-4381.
40. Cho, S., Duffin, R., Thielbeer, F., Bradley, M., Megson, I., Macnee, W., Poland, C., Tran, C. and Donaldson, K. (2012) Zeta Potential and Solubility to Toxic Ions as Mechanisms of Lung Inflammation Caused by Metal/Metal Oxide Nanoparticles. *Toxicol. Sci.* 126(2):469-477.
41. Cho, W., Rodger Duffin, R., Howie, S., Scotton, C., Wallace, W., Macnee, W., Bradley, M., Megson, I. and Donaldson, K. (2011) Progressive severe lung injury by zinc oxide nanoparticles; the role of Zn²⁺ dissolution inside lysosomes. *Part. Fibre Toxicol.* 8:27.
42. Valko, M., Rhodes, C., Moncol, J., Izakovic, M. and Mazur, M. (2006) Free radicals, metals and antioxidants in oxidative stress-induced cancer. *Chem Biol Interact* 160:1-40.
43. Valko, M., Morris, H. and Cronin, M. (2005) Metals, toxicity and oxidative stress. *Curr Med Chem.* 12:1161-1208.
44. Liu, J., Qu, W. and Kadiiska, M. (2009) Role of oxidative stress in cadmium toxicity and carcinogenesis. *Toxicol Appl Pharmacol.* 238:209-214.
45. Blomgran, R., Zheng, L. and Stendahl, O. (2007) Cathepsin-cleaved Bid promotes apoptosis in human neutrophils via oxidative stress-induced lysosomal membrane permeabilization. *J Leukoc Biol* 81:1213-1223.
46. Matsuyama, S., Llopis, J., Deveraux, Q., Tsien, R. and Reed, J. (2000) Changes in intramitochondrial and cytosolic pH: early events that modulate caspase activation during apoptosis. *Nat Cell Biol Toxicol.* 2(6):318-325.

47. Xie, Z., Schendel, S., Matsuyama, S. and Reed, J. (1998) Acidic pH promotes dimerization of bcl-2 family proteins. *Biochemistry*. 37:6410-6418.
48. Shaikh Za, Vu Tt and Zaman K (1999) Oxidative stress as a mechanism of chronic cadmium-induced hepatotoxicity and renal toxicity and protection by antioxidants. *Toxicol Appl Pharmacol* 154:256-263.
49. Schrand, A., Rahman, M., Hussain, S., Schlager, J., Smith, D. and Syed, A. (2010) Metal-based nanoparticles and their toxicity assessment. *Nanomed Nanobiotechnol*. 2:544-568.
50. El-Sharaky, A., Newairy, A., Badreldeen, M., Eweda, S. and Sheweita, S. (2007) Protective role of selenium against renal toxicity induced by cadmium in rats. *Toxicology* 235:185-193.
51. Sanders, M., Sebire, M., Sturve, J., Christian, P., Katsiadaki, I., Lyons, B., Sheahan, D., Weeks, J. and Feist, S. (2008) Exposure of sticklebacks (*Gasterosteus aculeatus*) to cadmium sulfide nanoparticles: biological effects and the importance of experimental design. *Mar Environ Res*. 66:161-163.
52. Wang, L., Nagesha, D., Selvarasah, S., Dokmeci, M. and Carrier, R. (2008) Toxicity of CdSe Nanoparticles in Caco-2 Cell Cultures. *J Nanobiotechnology*. 6:11.
53. Zhang, Y., Chen, W., Zhang, J., Liu, J., Chen, G. and Pope, C. (2007) In vitro and in vivo toxicity of CdTe nanoparticles. *J Nanosci Nanotechnol* 7:497-503.
54. Lin, W., Xu, Y., Huang, C., Ma, Y., Shannon, K., Chen, D. and Huang, Y. (2009) Toxicity of nano- and micro-sized ZnO particles in human lung epithelial cells. *J Nanoparticle Res*. 11:25-39.
55. Song, W., Zhang, J., Guo, J., Ding, F., Li, L. and Sun, Z. (2010) Role of the dissolved zinc ion and reactive oxygen species in cytotoxicity of ZnO nanoparticles. *Toxicol Lett*. 199:389-397.
56. Yang, H., Liu, C., Yang, D., Zhang, H. and Xi, Z. (2009) Comparative study of cytotoxicity, oxidative stress and genotoxicity induced by four typical nanomaterials: the role of particle size, shape and composition. *J Appl Toxicol* 29:69-78.
57. Buelna-Chontal, M. and Zazueta, C. (2013) Redox activation of Nrf2 and NF- κ B: A double end sword? *Cell signalling*. 25(12):2548-2557.
58. Eom HJ and Choi J (2009) Oxidative stress of CeO₂ nanoparticles via p38-Nrf-2 signaling pathway in human bronchial epithelial cell, Beas-2B. *Toxicol Lett*. 187:77-83.
59. Braydich-Stolle, L., Schaeublin, N., Murdock, R., Jiang, J., Biswas, P., Schlager, J. and Hussain, S. (2009) Crystal structure mediates mode of cell death in TiO₂ nanotoxicity. *J Nanoparticle Res*. 11:1361-1374.

60. Pujalte I, Passagne I, Brouillaud B, Treguer M, Durand E, Ohayon-Courtes C and L'azou B (2011) Cytotoxicity and oxidative stress induced by different metallic nanoparticles on human kidney cells. *Part Fibre Toxicol.* 8:10.
61. Ohayon-Courtès, C., Passagne, I., De Portal, C., Pouvreau, C., Cambar, J. and L'azou, B. (2007) ICP/OES application for assessing cadmium uptake (or toxicity) in glomerular cells: influence of extracellular calcium. *J. Toxicol. Environ. Health. Part A.* 70:750-759.
62. Gunness, P., Aleksa, K., Kosuge, K. and Ito, S. (2010) Comparison of the novel HK-2 human renal proximal tubular cell line with the standard LLC-PK1 cell line in studying drug-induced nephrotoxicity. *Can J Physiol Pharmacol.* 88:448-455.
63. Racusen, L., Monteil, C., Sgrignoli, A., Lucskay, M., Marouillat, S., Rhim, J. and Morin, J. (1997) Cell lines with extended in vitro growth potential from human renal proximal tubule: characterization, response to inducers, and comparison with established cell lines. *J Lab Clin Med.* 129:318-329.
64. Ryan, M., Johnson, G., Kirk, J., Fuerstenberg, S., Zager, R. and Torok-Storb, B. (1994) HK-2: an immortalized proximal tubule epithelial cell line from normal adult human kidney. *Kidney Int.* 45:48-57.
65. Sohaebuddin, S., Thevenot, P., Baker, D., Eaton, J. and Tang, L. (2010) Nanomaterial cytotoxicity is composition, size, and cell type dependent. *Part Fibre Toxicol* 7:22.

Table 1: Physicochemical parameters of TiO₂, ZnO and CdS nanoparticles

Particles	Source	Average diameter (TEM) [nm ± sd]	Shape (MET)	Specific surface area [m ² /g]	Zeta potentiel in RPMI [mV ± sd]	Crystal structure
TiO ₂	Sigma Aldrich	12 ± 2	spherical	63	-17,8 ± 4,4	Anatase
ZnO	Sigma Aldrich	75 ± 19	heterogeneous	7 - 14	-26,8 ± 4,5	Zincite
CdS	ICMCB	8 ± 1	spherical	80	-28,5 ± 3,3	Hexagonal

Experiments were performed in RPMI 1640-serum free. Data were derived and summarized from previous study¹⁷

Table 2: PCR Conditions and Primers used

	F	R	T	N Cycles
Heme oxygenase (HO-1)	TCCTTACCGTGGGCACTGAA	CACCCACGCATGGCTCAAAA	56 °C	35 cycles
Catalase (CAT)	TCGACCCAAGCAACATGCCA	ACGCTAAGCTTCGCTGCACA	56 °C	34 cycles
Thioredoxin reductase (TRNX-R)	AACCACTGGCTCGTTTCCGT	AGGCAATGGCTGGCCAAGTA	58 °C	35 cycles
Superoxyde dismutase (SOD-1):	TGGGGTTTCCGTTGAGTCCT	ACCACAAGCCAAACGACTTCCA	58 °C	32 cycles
Glutathion peroxidase (GPX-1)	TTCGAGCCCAACTTCATGCTCT	TGCTGACACCCGGCACTTTATT	58 °C	32 cycles
Glutathion-S-transférase (GST-pi)	CTCACTCAAAGCCTCCTGCCTAT	CAGGATGGTATTGGACTGGTACAG	60 °C	32 cycles
Actin-β (ACT-β)	GGCATCGTGATGGACTCCG	GCTGGAAGGTGGACAGCGA	57 °C	21 cycles

PCR primers, amplicon size, temperature of hybridization and number of amplification cycles.

FIGURE LEGENDS

Figure 1: Soluble fraction of dissolved metal in the supernatant of TiO₂, ZnO, and CdS NP suspensions. Determination of soluble metal was performed by ICP-OES from different concentrations of NPs 0, 2, 4, 8 and 16 µg /ml in RPMI 1640-serum-free medium; ZnO (light grey line), CdS (grey line) and TiO₂ (black line) for 0 (discontinuous line) or 24 h (continuous line). Data shown are means, ± se (N>3). The TiO₂ dissolution curves are overlapped.

Figure 2: Cytotoxicity of NPs. Cytotoxicity was investigated using the WST-1 assay. After 24 h exposure, the cytotoxic effects of NPs (ZnO, CdS, and TiO₂) were compared to soluble (ZnCl₂ and CdO) and bulk forms (ZnO, CdS, and TiO₂ microparticles) (A, C and E respectively), and to a suspension of ZnO NPs with EDTA (B) and CdS NPs with EDTA (50 µM) (D). Data shown are means ± se (N>3).

Figure 3: ROS production related with NP exposure. ROS production on HK-2 cells induced by TiO₂, ZnO, and CdS on the HK-2 cell line was investigated using DCFH-DA assay (A). Cells were exposed 4 h in RPMI 1640- serum-free medium containing different concentration of NPs: TiO₂ (5 and 20 µg /cm²), ZnO (1.5 and 20 µg /cm²) and CdS (2.8 and 5.6 µg /cm²). Data shown are means ± se of at least three independent experiments and expressed as the percentage of the ROS level compared to control group. *Significant difference with respect to control (p<0.05). The importance of NP-induced ROS formation on cell mortality was evaluated using the WST-1 assay. Cells were incubated with different concentrations of ZnO NPs (2.6, 5.2, and 10 µg/cm²) (B) and CdS NPs (3.5, 5.2, and 7 µg/cm²) coincubated with 10 mM NAC (N>3) (C).

Figure 4: Lipid peroxidation after NP exposure. Lipid peroxidation was assessed via measurement of MDA in cells after 24h exposure to NPs (20 µg /cm² TiO₂ NPs, 2 µg /cm² ZnO NPs and 5 µg /cm² CdS NPs) using the TBARS assay. TBHP (50 µM) was used as positive control. Cellular MDA levels were assessed. Data shown are means ± se (N=3). *Significant difference with respect to control (p<0.05).

Figure 5: Lysosomal membrane destabilization: Lysosomal membrane destabilization was visualized (A) and quantified (B) via acridine orange staining in cells exposed to NPs ($20 \mu\text{g}/\text{cm}^2$ TiO₂ NPs, $2 \mu\text{g}/\text{cm}^2$ ZnO NPs, and $5 \mu\text{g}/\text{cm}^2$ CdS NPs) for 24 h as compared to control. In healthy cells, lysosomes can be seen as red-orange granules and the cytoplasm has diffuse green fluorescence. In cells with lysosomal membrane damage, lysosomes exhibit a shift from red-orange to a green color and overall intensity of green fluorescence is increased in such cells. TBHP ($50 \mu\text{M}$) was used as positive control. *Significant difference with respect to control ($p < 0.05$).

Figure 6: Nuclear condensation. Nuclear condensation was determined by DAPI staining. Cells were exposed to different concentration of NPs ($0.2, 2,$ and $20 \mu\text{g}/\text{cm}^2$ for TiO₂ NPs; $0.02, 0.2,$ and $2 \mu\text{g}/\text{cm}^2$ for ZnO NPs; $2.8, 4.2,$ and $6.35 \mu\text{g}/\text{cm}^2$ for CdS NPs) for 24 h. Representative images were obtained with $20 \mu\text{g}/\text{cm}^2$ TiO₂ NPs, $2 \mu\text{g}/\text{cm}^2$ ZnO NPs, and $6.35 \mu\text{g}/\text{cm}^2$ CdS NPs (A). Cells having condensed nuclei were considered in a state apoptosis. Cells were photographed and percentage of cells with apoptotic nuclei were determined under blinded scoring, $N > 100$ (B). *Significant difference with respect to the control ($p < 0.05$).

Figure 7: Expression of Nrf2 and NF- κ B in cytosolic and nuclear fractions of cells. Cells were exposed to TiO₂ ($20 \mu\text{g}/\text{cm}^2$), ZnO ($2 \mu\text{g}/\text{cm}^2$) and CdS ($5 \mu\text{g}/\text{cm}^2$) NPs for 1 and 4 h. Densitometric values of nuclear and cytosolic expression of Nrf2 (A) and NF- κ B (B) were obtained by Western blot and normalized using that of α -Tubulin (cytosolic fraction) and TBP (nuclear fraction) and presented as units compared to the control. Data shown are means \pm se ($N > 3$).

Figure 8: Induction of oxidative stress-related genes. Cells were treated with to TiO₂ ($20 \mu\text{g}/\text{cm}^2$), ZnO ($2 \mu\text{g}/\text{cm}^2$) and CdS ($5 \mu\text{g}/\text{cm}^2$) NPs for 24 h. mRNA transcription was detected using RT-PCR analysis and respective primers. Results were normalized using that actin, and presented as relative units compared to the control. Data shown are means \pm se ($N > 3$).

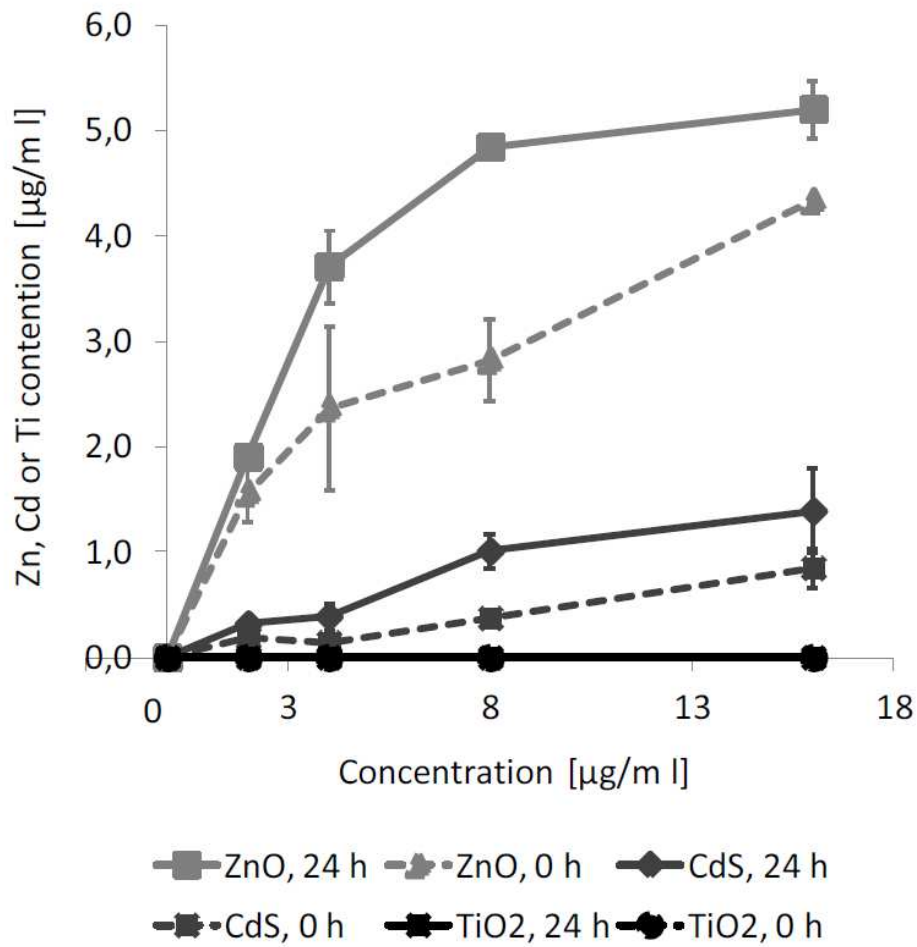


Figure 1

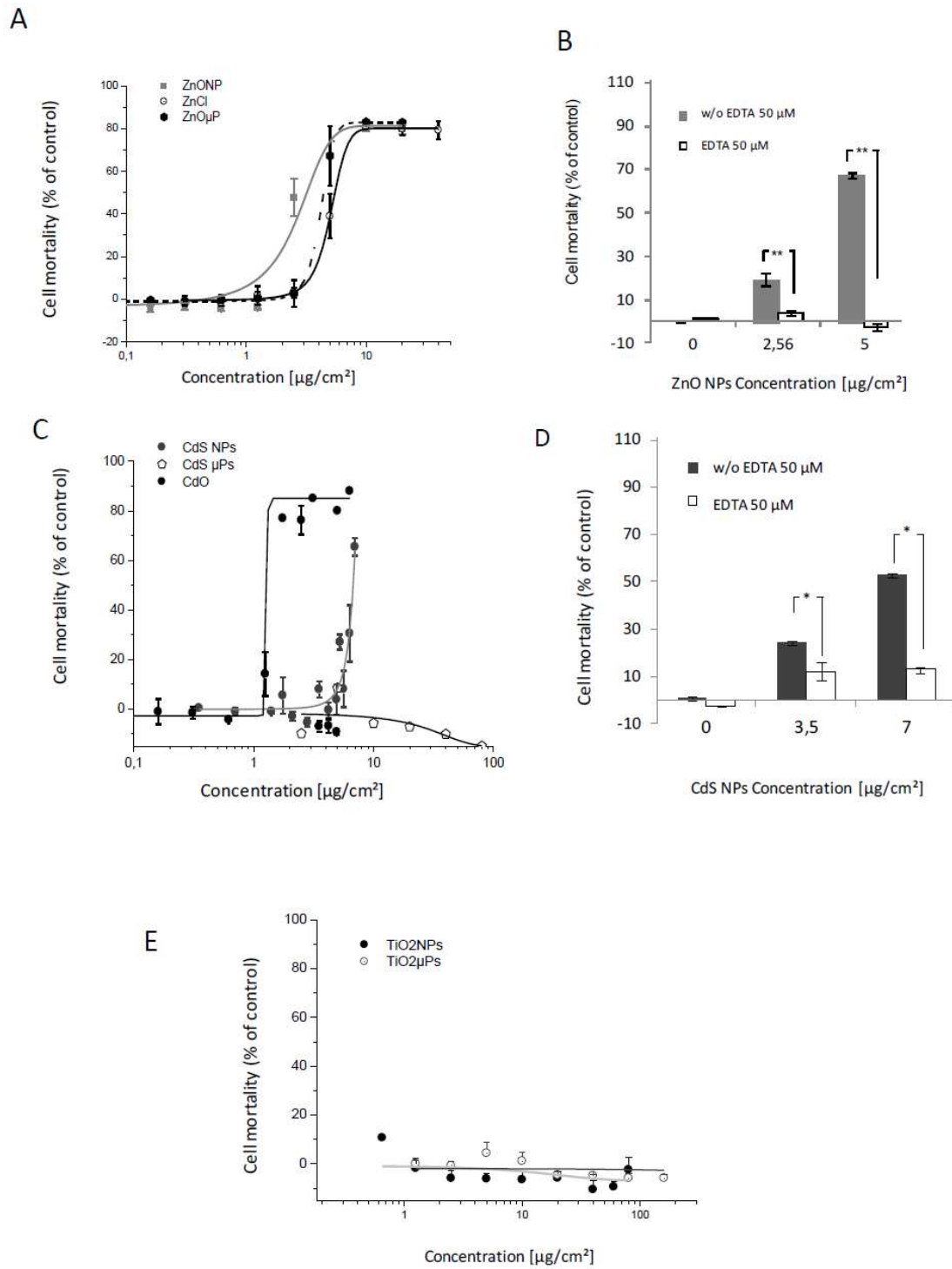


Figure 2

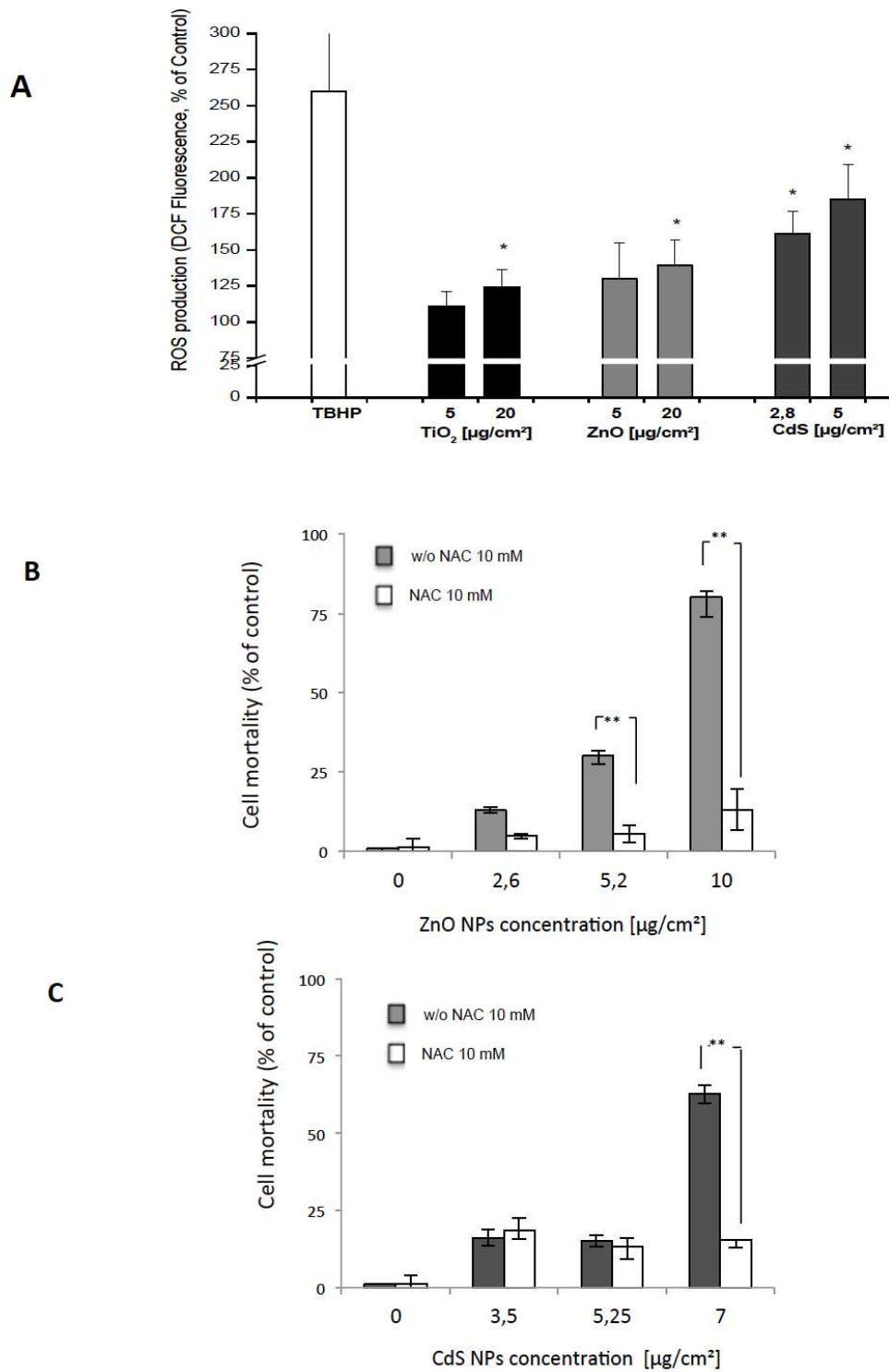


Figure 3

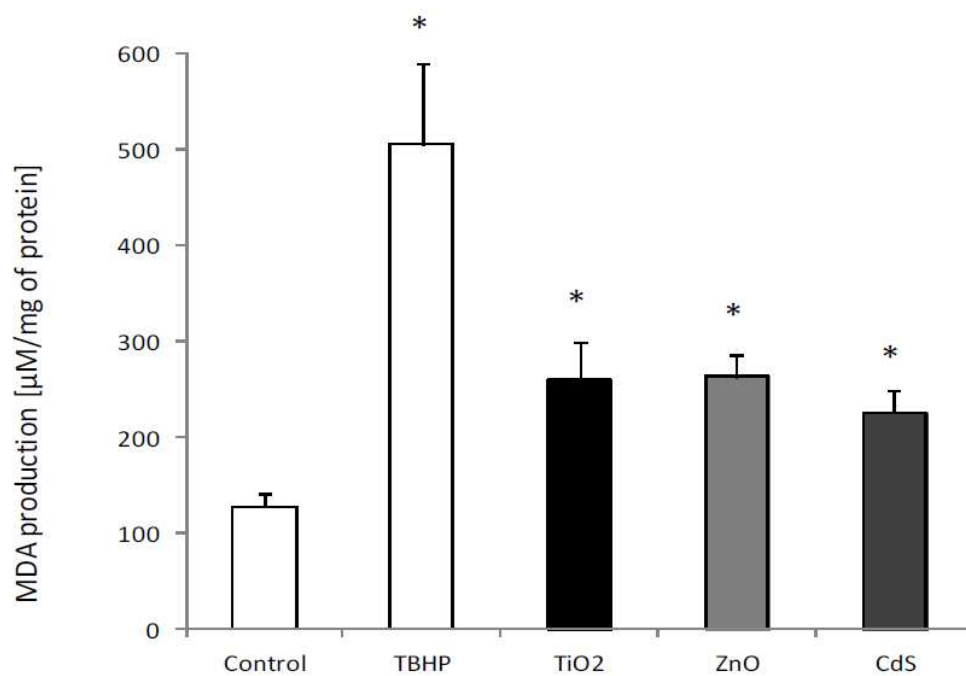


Figure 4

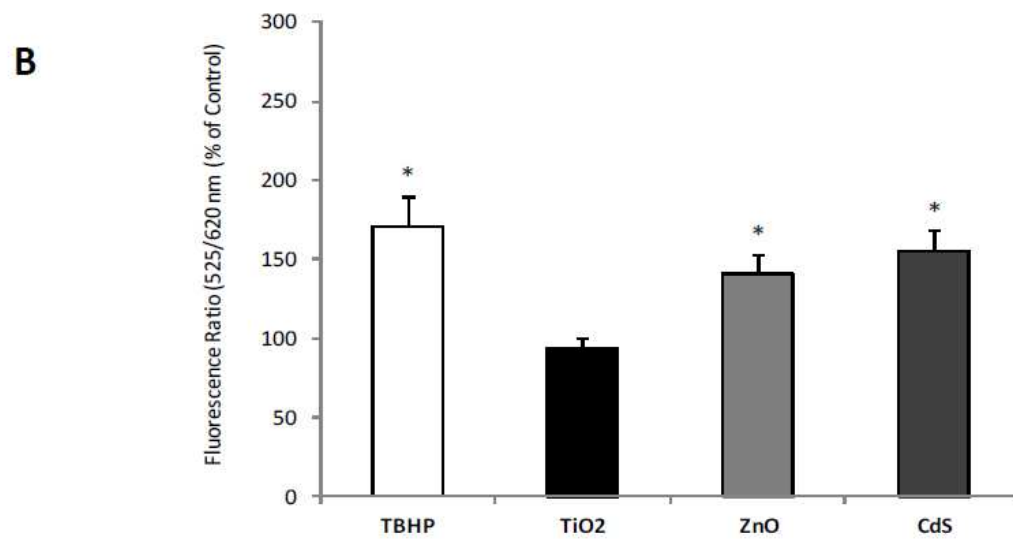
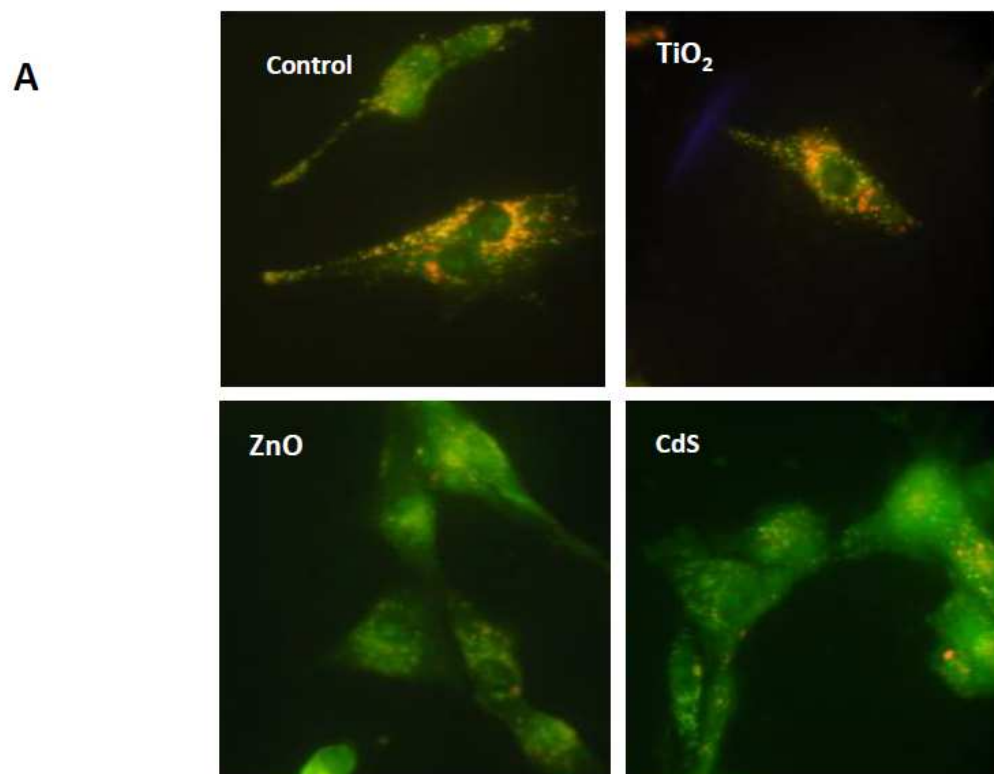


Figure 5

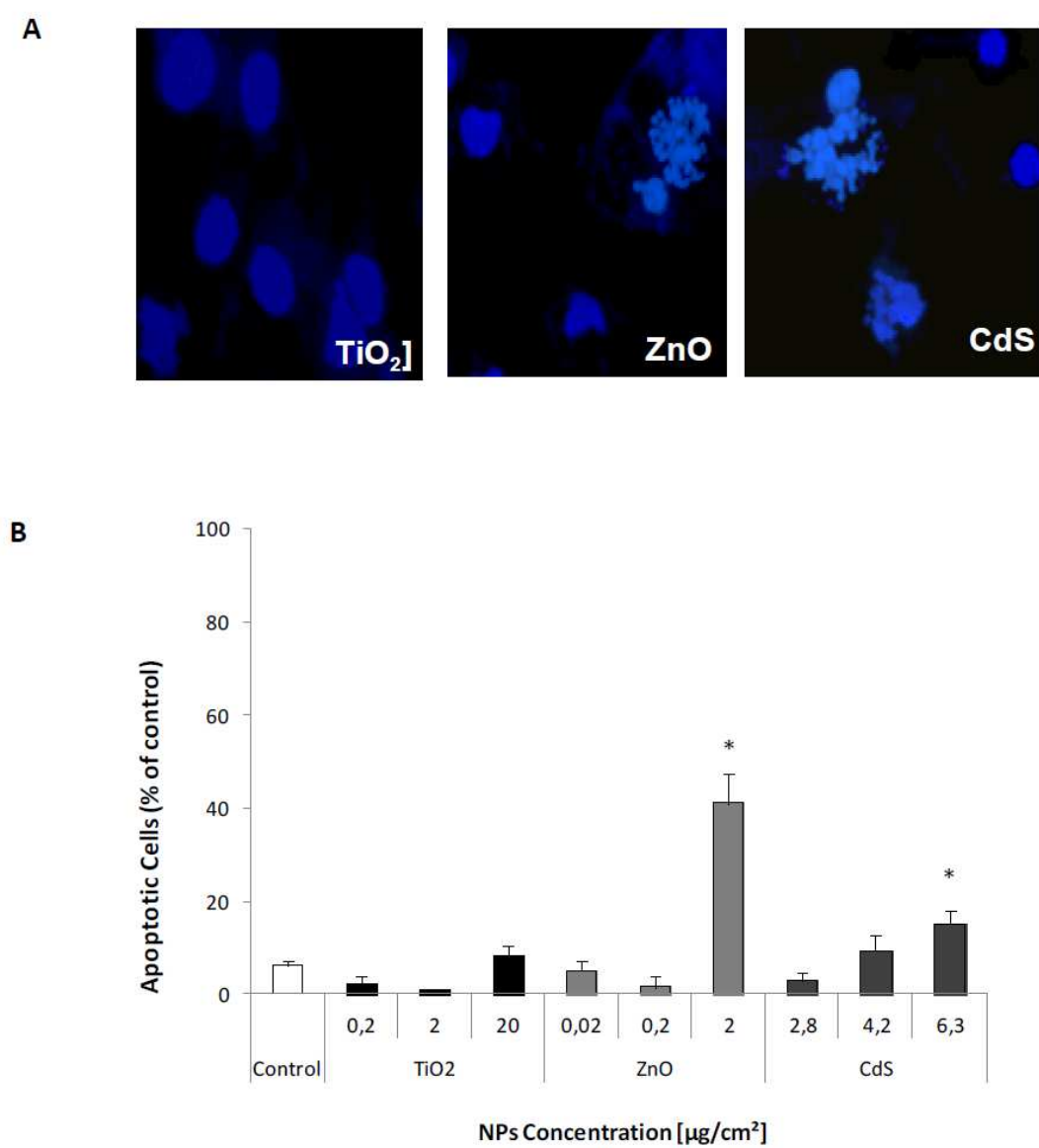


Figure 6

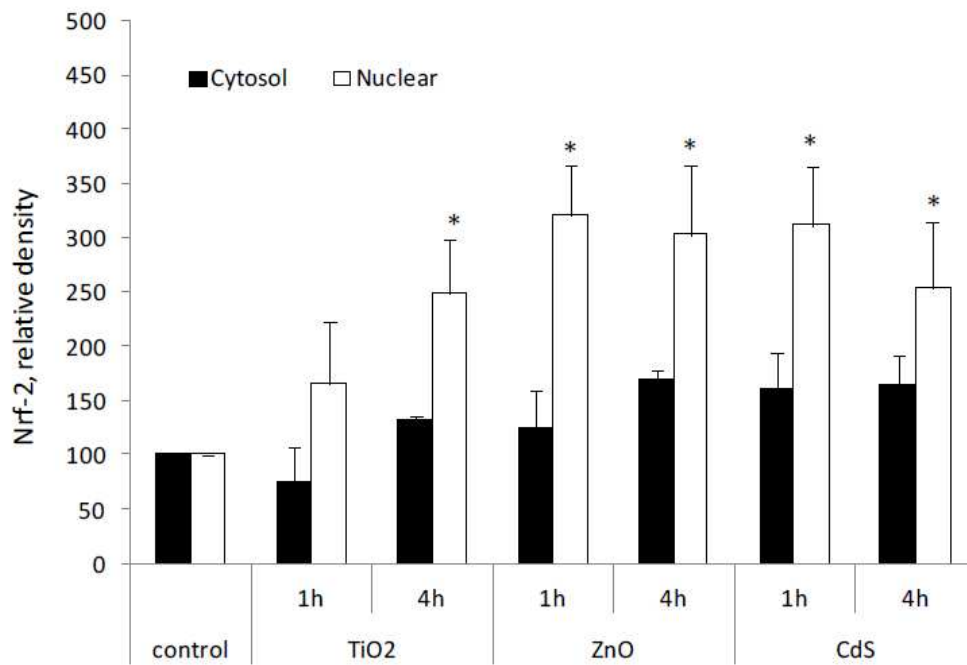
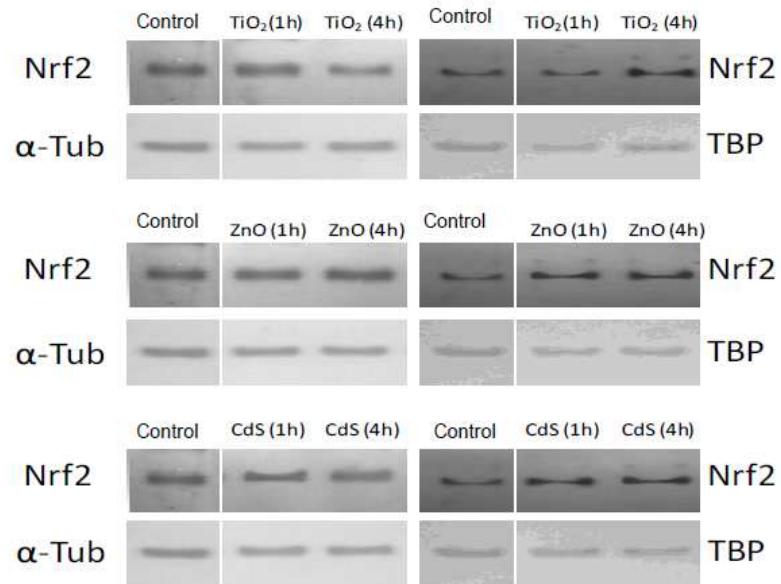


Figure 7A

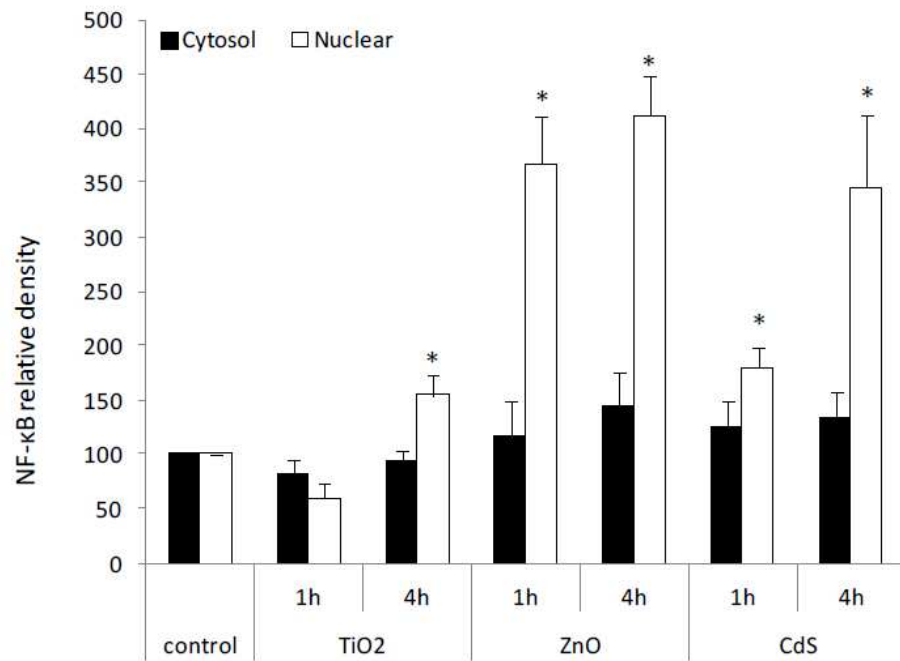
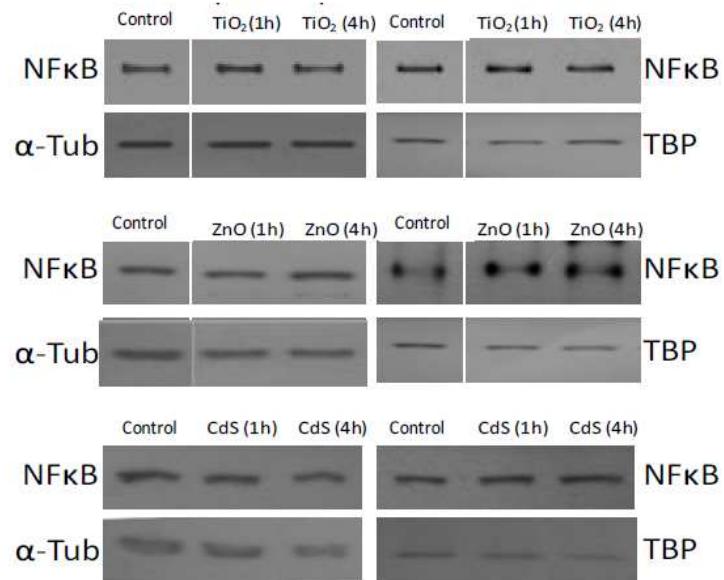


Figure 7B

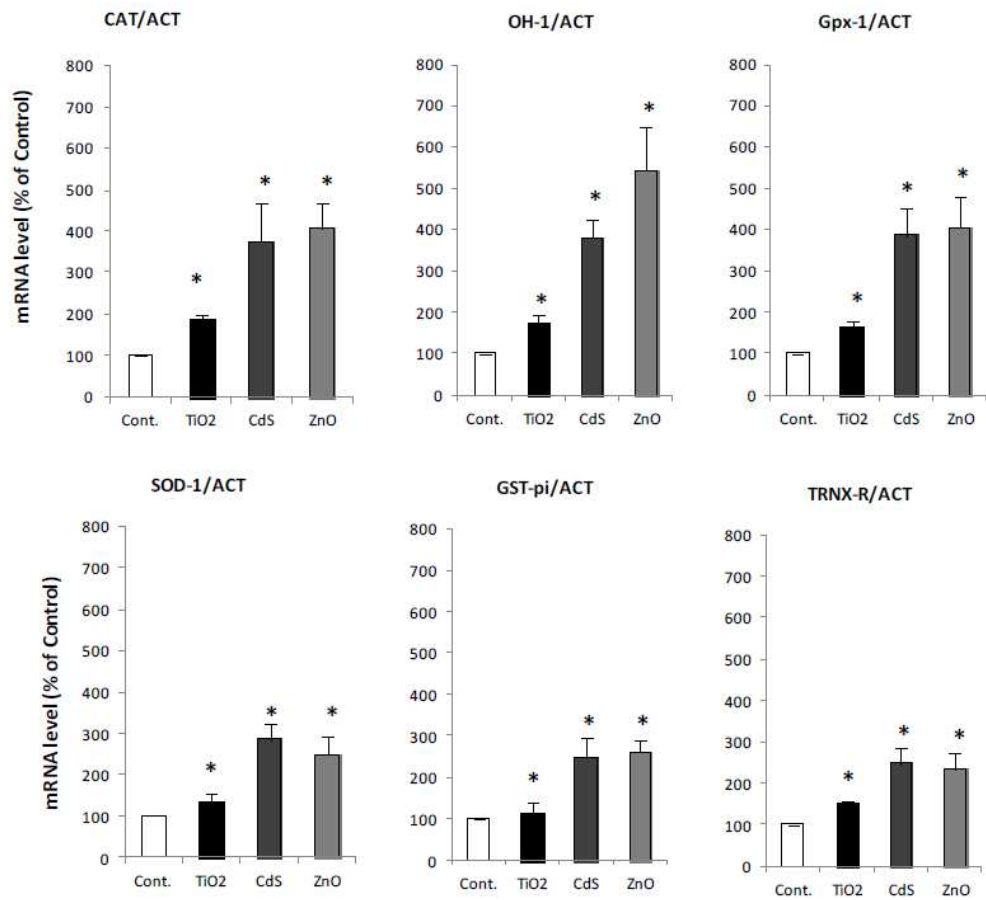


Figure 8